International Journal for Multidisciplinary Research (IJFMR)
E-ISSN: 2582-2160 ● Website: www.ijfmr.com ● Email: editor@ijfmr.com

Behaviour of Whitcomb Integral Supercritical Airfoil at Various Angles of Attack in Sonic Condition Using CFD

S. Shawn Varghese[1], L.S Madhumitha[2]

[1,2]Department of Aerospace Engineering, Hindustan Institute of Technology and Science, Chennai, Tamil Nadu, India

Abstract

Understanding the aerodynamic behaviour of an airfoil is crucial for evaluating its performance in generating lift and drag. In this study, the aerodynamic performance of the Whitcomb Integral Supercritical Airfoil is analysed across a range of angles of attack—specifically, 2°, 4°, 6°, 8°, and 10°—under sonic conditions. The primary objective is to investigate and characterize the lift and drag properties exhibited by the airfoil at these various angles of attack. This analysis will provide insights into how the airfoil performs in terms of efficiency and stability at sonic speeds.

Keywords: Airfoil, CFD, lift, drag, angle of attack, pressure, temperature, velocity inlet, Whitcomb integral supercritical airfoil, Ansys.

1. INTRODUCTION

In the 1960s, the National Advisory Committee for Aeronautics (NACA), which later became part of NASA, was actively engaged in research to address the challenges associated with transonic flight, particularly within the Mach 0.8 to 1.2 range. This speed range is characterized by a significant increase in drag due to the formation of shock waves, a phenomenon known as wave drag. One of the most notable outcomes of this research was the development of the supercritical airfoil, a pioneering design introduced by Dr. Richard Whitcomb, a leading NACA engineer [1].

The supercritical airfoil was specifically engineered to mitigate the adverse effects of wave drag, which conventional airfoil designs struggle with as aircraft approach the speed of sound. Unlike traditional airfoils, which have a more rounded upper surface that accelerates airflow and induces early shock wave formation, the supercritical airfoil features a flatter upper surface. This design reduces the acceleration of airflow over the wing, thereby delaying the onset of shock waves and minimizing wave drag [2].

Additionally, the supercritical airfoil incorporates a more pronounced camber in its aft section, facilitating smoother pressure recovery behind the shock wave and enhancing the lift-to-drag ratio — an essential flight at high speeds. The airfoil's thicker cross-section also enables the construction of stronger and lighter wing structures, a critical consideration in aircraft design.

This innovative airfoil design not only significantly reduces drag but also improves the overall aerodynamic efficiency and fuel economy of aircraft operating in the transonic and low supersonic speed ranges. The supercritical airfoil represents a major advancement in aerodynamics, forming the basis for the design of modern high-speed aircraft and contributing to their enhanced performance and efficiency.

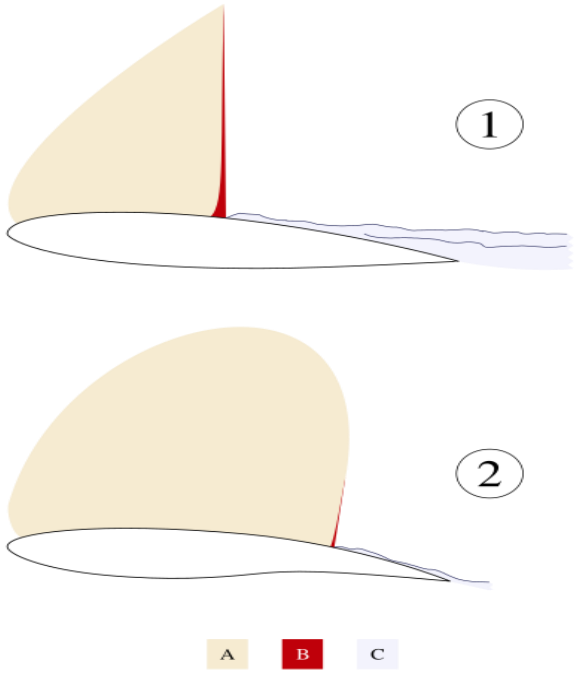

Figure 1 conventional (1) and supercritical (2) airfoils at identical free stream Mach number. Illustrated are: A – supersonic flow region, B – shock wave, C – area of separated flow. The supersonic flow over a supercritical airfoil terminates in a weaker shock [4].

2. METHODOLOGY

The airfoil was modelled and meshed in two dimensions using ANSYS software, enabling a comprehensive computational analysis. Simulations were performed in ANSYS Fluent at various angles of attack, specifically at 2°, 4°, 6°, 8°, and 10°. An inlet velocity of 330 m/s, representative of sonic conditions, was applied for each angle of attack during the analyses.

From the computational analysis, the coefficients of lift (C_l) and drag (C_d) were obtained for the Whitcomb Integral Supercritical Airfoil. These coefficients are essential for understanding the aerodynamic performance of the airfoil. Furthermore, the lift-to-drag ratio was calculated to evaluate the airfoil's efficiency under the specified conditions. This ratio serves as a critical metric in aerodynamic design, indicating the effectiveness with which the airfoil generates lift in relation to the drag it produces. In summary, this study aims to advance the understanding of the aerodynamic characteristics of the Whitcomb Integral Supercritical Airfoil, providing valuable data that can inform future aircraft design and enhance performance optimization efforts.

2.1 AIRFOIL SPECIFICATIONS

Name of the Airfoil	Whitcomb Integrated supercritical airfoil
Maximum Thickness	11 % at 35 % chord
Maximum Camber	2.4 % at 82.5 % chord
Chord length	1 m

Table 1 Airfoil specifications

2.2 DESIGN AND GENERATION OF WHITCOMB SUPERCRITICAL AIRFOIL

The coordinates are generated as a "CSV file of coordinates" using the Airfoil Plotter tool. The initial geometry is created using ANSYS Workbench R24.1. ANSYS, an American public company established in 1970, specializes in Computer-Aided Engineering (CAE) software widely used across various industries for analysing real-time flow fields around objects and determining aerodynamic forces such as lift and drag. Moreover, ANSYS facilitates the simulation of airflow over airfoils according to user-defined parameters, enabling the assessment of flow field characteristics and regions of stress concentration. The software offers exceptional accuracy, yielding results with up to 99.99% precision, attributable to its finely detailed meshing capabilities, which range from -100 to +100. Its user-friendly interface streamlines the process of creating 2D geometries through coordinate import and enables the development of 3D models by importing designs from any CAD software [1].

2.3 MODEL AND MESH OF AIRFOIL

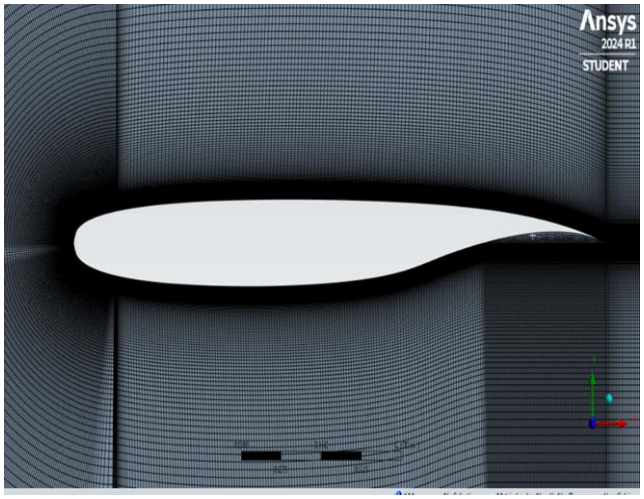

Figure 2 Meshing of Whitcomb SC airfoil

A computational domain has been established around the airfoils for the analysis, as illustrated in the image below.

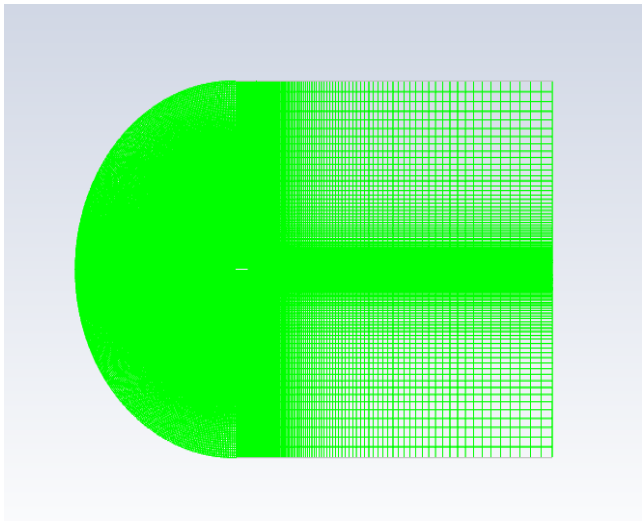

Figure 3 C- type computational domain around airfoil

2.4 OPERATING CONDITIONS AND REYNOLDS NUMBER

The simulations were performed under standard room temperature conditions, set at 27°C (300 K). Dry air was selected as the fluid medium for these analyses. The specific properties of dry air used in the simulations, including density, viscosity, and other relevant parameters, are provided in the accompanying table below. This choice of fluid medium and temperature is intended to replicate typical atmospheric conditions.

Operating Temperature	300 K
Operating Pressure	101325 Pa
Fluid	Dry air
Viscosity of air (μ) at 300 K	18.46×10^{-6} kg/m-s
Density of air (ρ) at 300 K	1.177 kg/m^3
Specific Heat (C_p) at 300 K	1.006 kJ/kg-K
Thermal Conductivity (k) at 300 K	0.02624 w/m-K

Table 2 Operating conditions

2.5 PROBLEM SETUP, BOUNDARY CONDITIONS AND SOLUTION METHOD

SOLVER	
Solver Type	Density Based
Time	Steady
Velocity formulation	Absolute
2D Space	Planar
Multiphase	Off
Energy	On
Viscous model	K omega
K omega model	SST

Table 3 Solver Conditions

BOUNDARY CONDITIONS	
Inlet type	Velocity inlet
Outlet type	Pressure outlet

Table 4 Boundary Conditions

SOLUTION METHOD	
Pressure velocity coupling scheme	Coupled
Gradient	Green-Gauss Node based
Pressure	Second order
Momentum	Second order Upwind solution
Initialization	From velocity inlet

Table 5 Solution Method

The lift and drag forces acting on airfoils are essential parameters in aerodynamics, which can be quantified using specific equations, The lift force (F_L) is calculated as:

$$F_L = 12\rho V^2 A C_L$$

Where,

ρ represents the air density, V is the velocity of the airflow, A is the planform area of the airfoil, and C_L is the coefficient of lift for the airfoil shape. Conversely, the drag force (F_D) is determined by the equation:

$$F_D = 12\rho V^2 A C_D$$

Where,

C_D is the coefficient of drag. In our case, the planform area (A) is 1 m2, which corresponds to an airfoil with a chord length of 1 m and a wingspan of 1 m.

3. RESULTS

1. AT 0º AOA

a) Velocity magnitude

From the CFD analysis of the Whitcomb integral supercritical airfoil at 0º angle of attack, an increase in velocity on the suction or upper surface of the airfoil is observed, while the velocity decreases on the lower surface. A similar pattern of velocity changes is evident near the leading edge and the cusp region of the trailing edge. In these areas, a low-velocity region exists close to the surface of the leading and trailing edges, with velocity increasing slightly as it moves further into the flow.

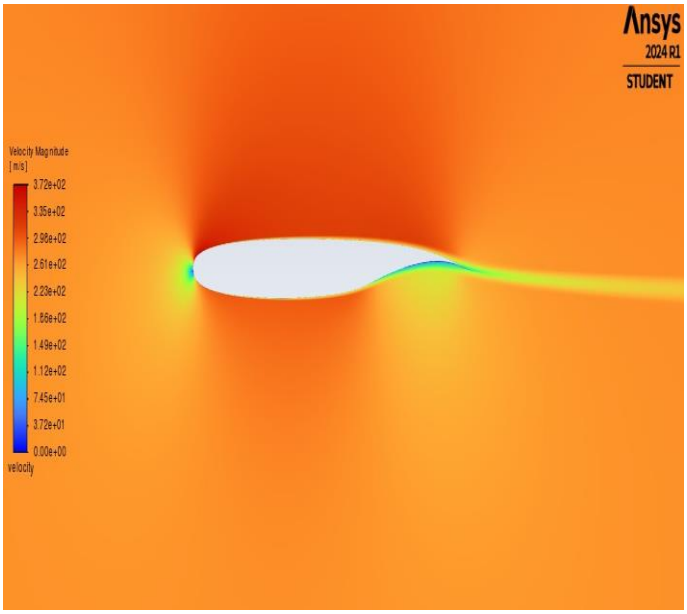

Figure 4 Velocity magnitude contour at 0º AOA

b) Static pressure

The figure below illustrates that the upper surface of the airfoil is a low-pressure region, while there is a slight increase in pressure on the lower surface. At the leading edge, there is a significant increase in pressure, whereas in the cusp region, the pressure is slightly lower compared to the leading edge.

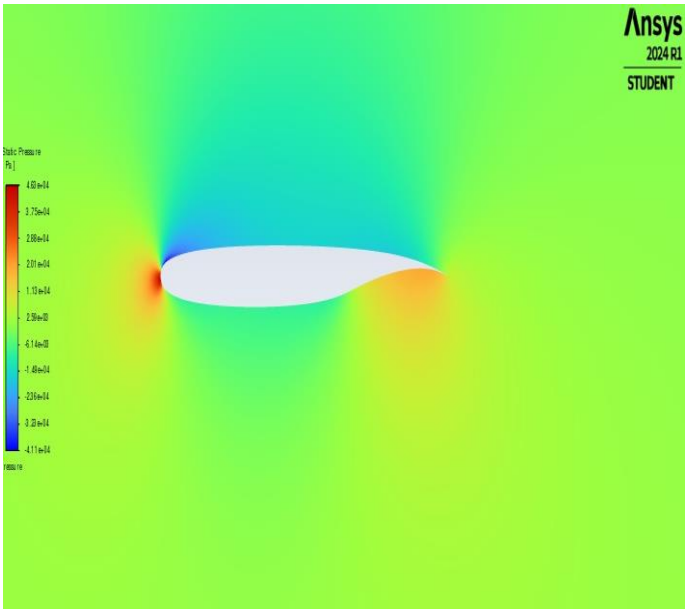

Figure 5 Static pressure contour at 0º AOA

2. AT 2º AOA

a) Velocity magnitude

It is evident that the upper surface of the airfoil is a high-velocity region, while the lower surface is a low-velocity region. A similar pattern of velocity changes, as observed at 0 angle of attack, is seen near the leading edge and the cusp of the trailing edge of the airfoil.

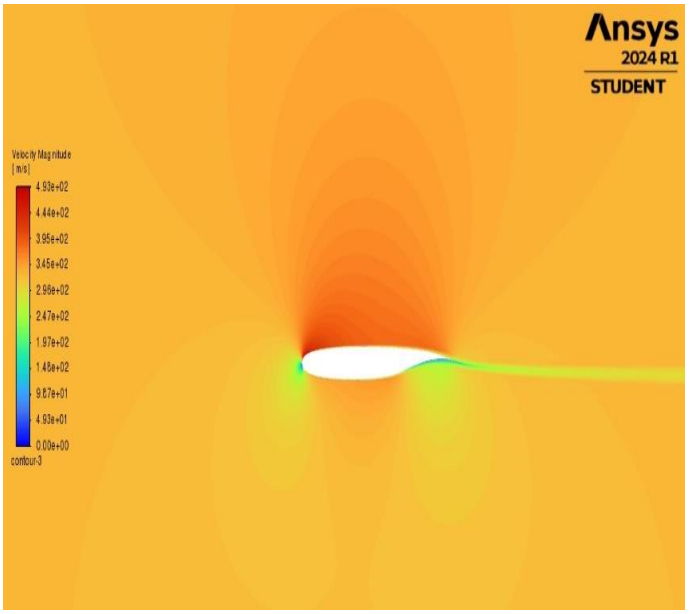

Figure 6 Velocity magnitude contour at 2° AOA

b) Static pressure

The upper surface of the airfoil exhibits significantly lower pressure, while the lower surface shows a region of moderate pressure. Higher pressure regions are observed at both the leading and trailing edges.

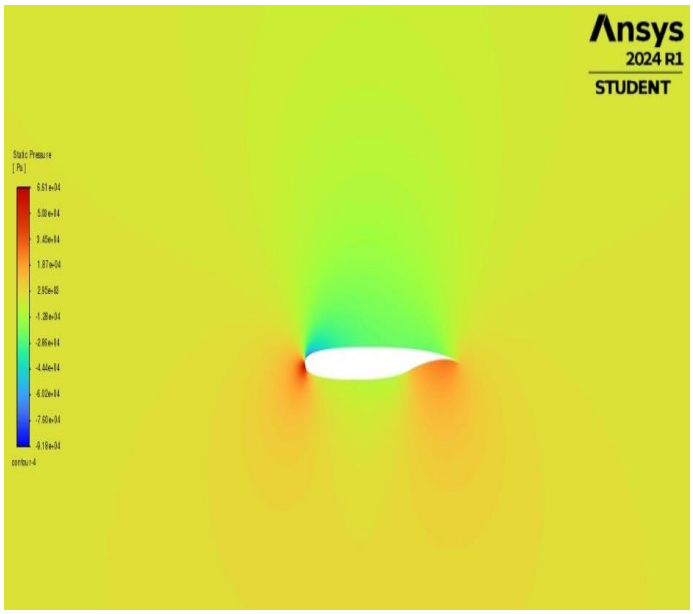

Figure 7 Static pressure contour at 2° AOA

3. AT 4º AOA

a) Velocity magnitude

The upper surface of the airfoil shows a higher velocity region, while the lower surface experiences a decrease in velocity. Near the leading and trailing edges, there are lower velocity regions close to the surface, with the velocity increasing to a moderate level as it moves into the flow.

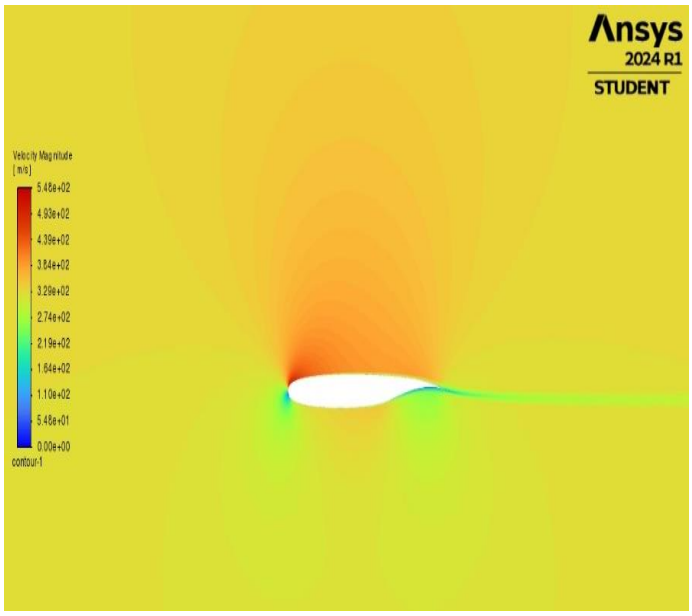

Figure 8 Velocity magnitude contour at 4º AOA

b) Static pressure

The leading and trailing edges exhibit higher pressure, which extends to the lower surface of the airfoil, where the pressure is above a moderate range. The upper surface has the lowest pressure region.

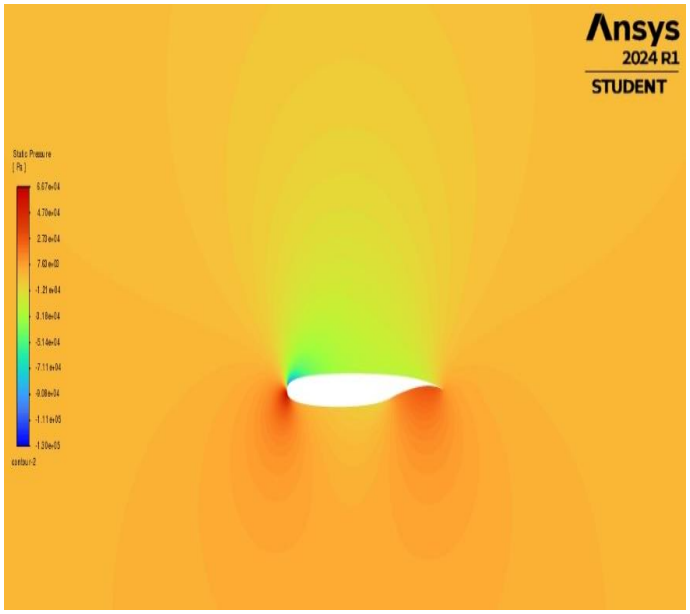

Figure 9 Static pressure contour at 4º AOA

4. AT 6º AOA

a) Velocity magnitude

The upper surface of the airfoil has a higher velocity region, while the lower surface shows a moderate range of velocity. The leading edge and cusp region exhibit the lowest velocity, with no further increase observed.

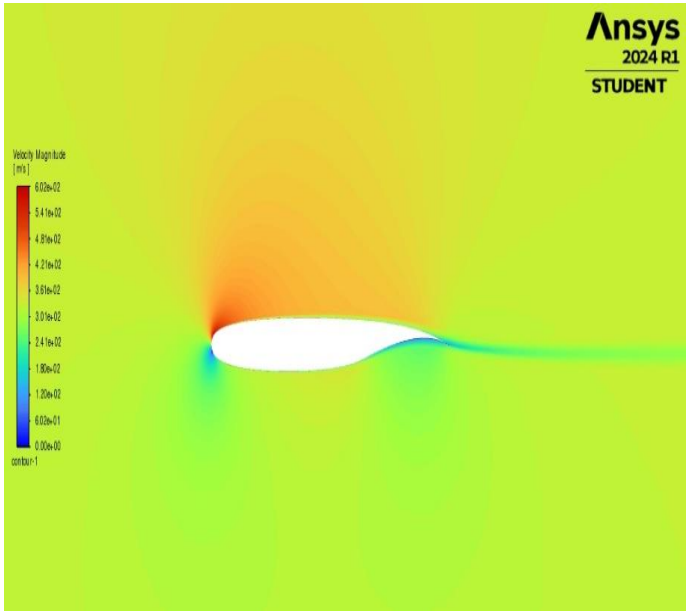

Figure 10 Velocity magnitude contour at 6º AOA

b) Static pressure

The pressure intensity is observed to be very high at the leading edge, lower surface, cusp region, and trailing edge. The upper surface of the airfoil has an average level of pressure.

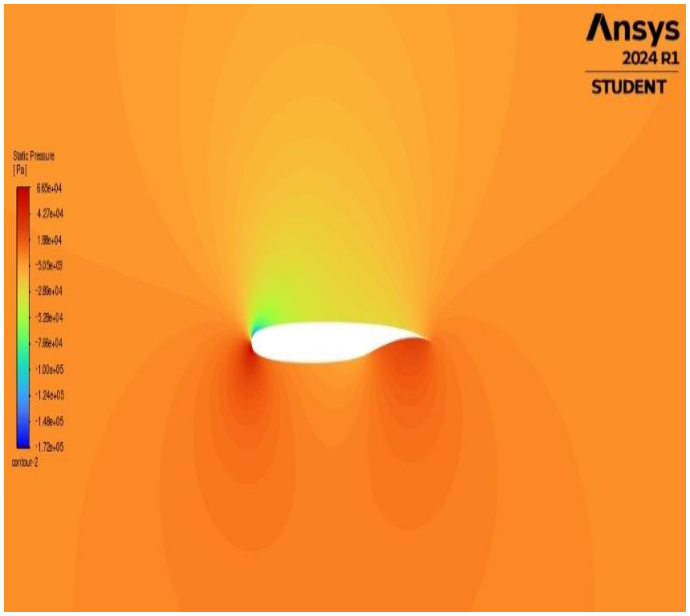

Figure 11 Static pressure contour at 6º AOA

5. AT 8º AOA

a) Velocity magnitude

The upper surface of the airfoil experiences higher velocity compared to the lower surface. At the leading and trailing edges of lower surface, the velocity is significantly low. On the upper surface, particularly at the leading edge, the velocity is much greater, gradually decreasing as it approaches the upper trailing edge.

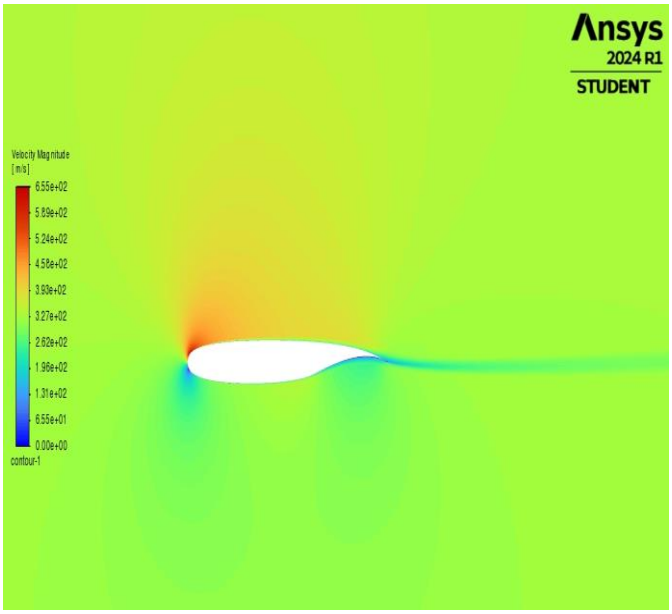

Figure 12 Velocity magnitude contour at 8º AOA

***b)* Static pressure**

The lower surface of the airfoil experiences a greater increase in pressure, while the upper surface displays lower static pressure. Notably, at the leading edge of the upper surface, the pressure is particularly low.

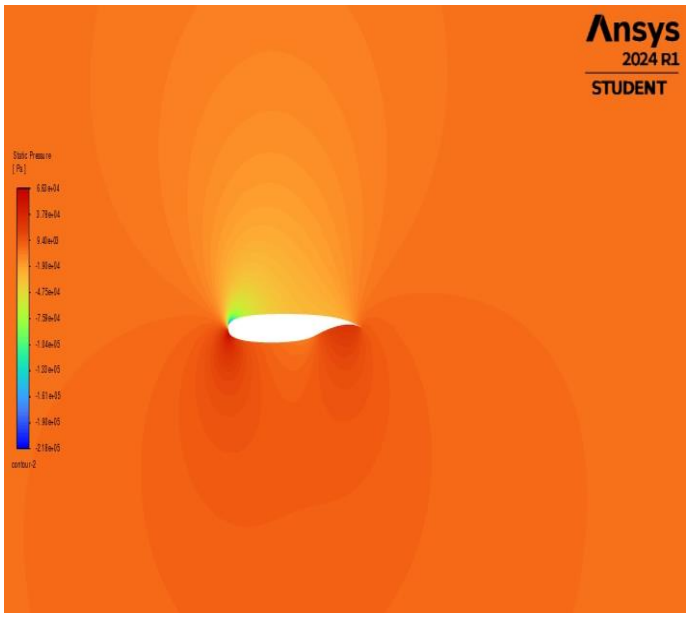

Figure 13 Static pressure contour at 8º AOA

6. AT 10º AOA

a) Velocity magnitude

The velocity is noticeably lower on the lower surface of the airfoil and higher on the upper surface. At both the leading edge and the cusp of the trailing edge, the velocity appears to be very low.

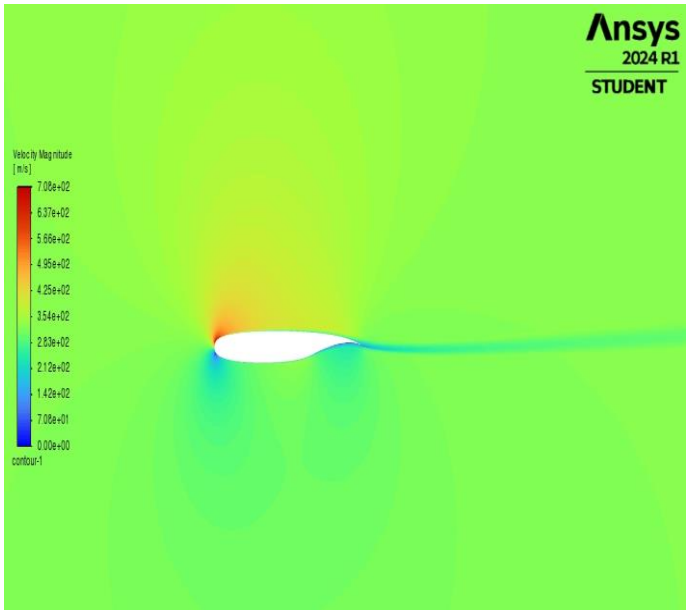

Figure 14 Static pressure contour at 10º AOA

b) Static pressure

The static pressure is significantly high on the lower surface, while on the upper surface, it is notably low, especially at the leading edge.

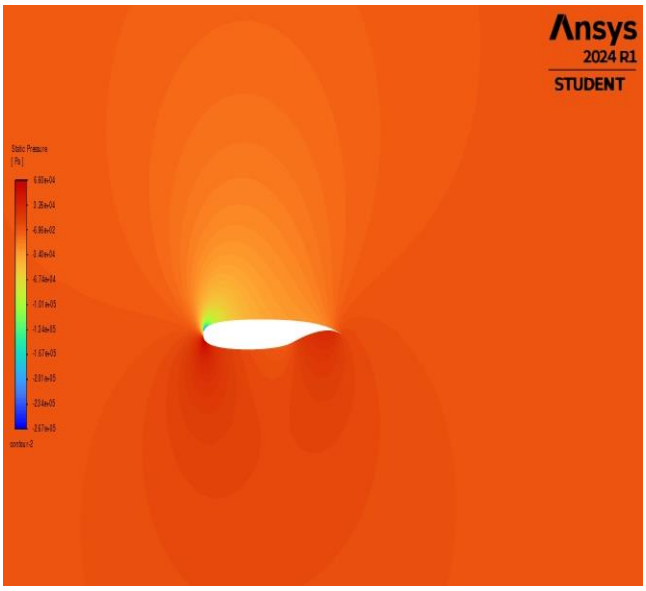

Figure 15 Static pressure contour at 10º AOA

AOA (DEGREE)	LIFT (N)	DRAG (N)	LIFT COEFFICIENT (C_L)	DRAG COEFFICIENT (C_D)	L/D RATIO
0	27577.30	577.02	0.3827	0.008	45.8375
2	32943.27	1093.29	0.4572	0.0152	30.13
4	40311	632.71	0.6044	0.0095	64.711
6	47447	3023.66	0.7114	0.045	15.87
8	61399.57	3673.15	0.9206	0.0551	16.715
10	61233.88	5814.77	0.9181	0.0872	10.531

Table 6 The table represents the maximum values obtained

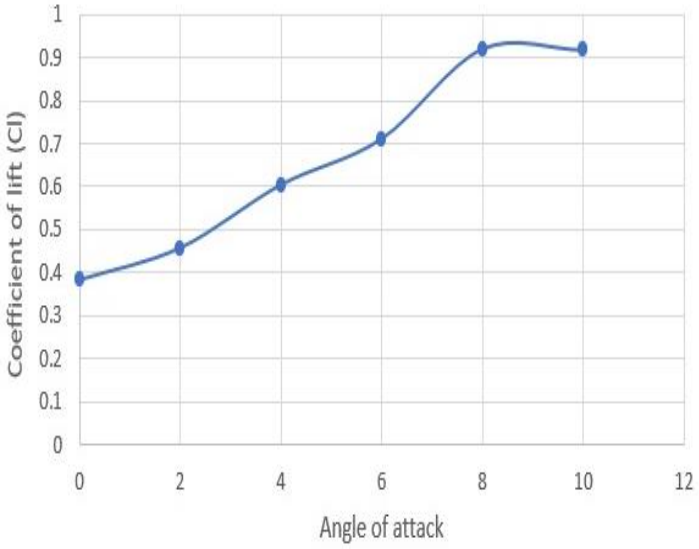

Figure 16 AOA vs C_L graph

The graph illustrates the relationship between the coefficient of lift (C_L) and the angle of attack (AOA) for a Whitcomb supercritical airfoil, highlighting its aerodynamic performance. As the angle of attack increases from 0º to 8º, there is a steady rise in the coefficient of lift. Initially, at an AOA of 0º, the C_L is approximately 0.35, and this value increases progressively with higher angles of attack.

At 8º AOA, the airfoil reaches its peak coefficient of lift, approximately 0.9. Beyond this point, when the AOA is increased to around 10º, the C_L stabilizes in the range of 0.88–0.9, indicating that the airfoil has reached its maximum lift-generating potential. This plateau suggests that the airfoil is approaching aerodynamic limitations, where further increases in AOA yield little to no additional lift, and the risk of flow separation and stall becomes imminent.

The operational efficiency of the Whitcomb supercritical airfoil is particularly notable within the AOA range of 6º to 8º. In this range, the airfoil demonstrates optimal lift production, aligning with its design goals of delaying the onset of shock-induced drag rise and improving performance at transonic speeds [6]. These characteristics underscore the airfoil's suitability for high-speed applications, as it mitigates the aerodynamic penalties typically associated with increased angles of attack and enables smoother, more efficient flight performance near the critical Mach number [7].

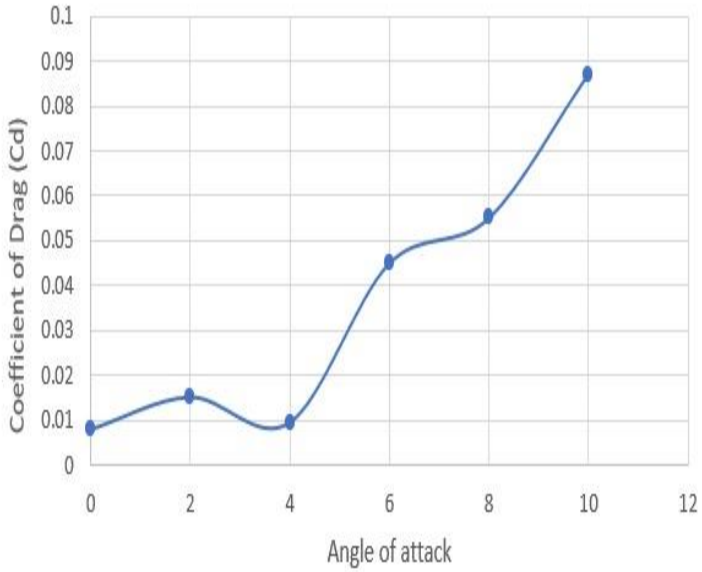

Figure 17 AOA vs C_D graph

The graph illustrates the correlation between the angle of attack and the coefficient of drag (C_D). In the initial range from 0º to approximately 3º, the C_d remains consistently low, varying between 0 and 0.02. This behaviour signifies minimal aerodynamic drag at low angles of attack, indicating that the airfoil operates efficiently within this range, encountering very little resistance. Such stability in drag suggests an optimal aerodynamic performance, where the airflow remains largely attached to the surface of the airfoil, contributing to lower drag force.

As the AOA increases beyond 4º, a distinct rise in the C_D becomes evident. This trend becomes even more pronounced beyond 6º, where the C_D exhibits a marked upward trajectory. Particularly between 8 º and 10 º, the drag coefficient experiences a sharp escalation, likely due to the onset of adverse aerodynamic phenomena such as flow separation or boundary layer thickening. These effects result in increased turbulent wake formation, significantly elevating the drag forces acting on the airfoil [8].

This observed trend underscores the airfoil's efficiency at lower AOA, where drag is minimized, and contrasts it with the substantial increase in drag as the angle of attack grows. The data suggests that, at higher angles, the airfoil becomes less aerodynamically efficient, likely as a consequence of increased flow disturbance and energy loss associated with boundary layer separation [7].

4. CONCLUSION

The CFD analysis of the Whitcomb integral supercritical airfoil provides insights into its aerodynamic behaviour across various angles of attack (AOA). At 0º AOA, the upper surface exhibits increased velocity and lower pressure, while the lower surface shows decreased velocity and a slight pressure increase. Low-velocity regions are present near the leading and trailing edges. As the angle of attack increases to 2º, 4º, 6º, 8º, and 10º, similar trends continue, with the upper surface consistently maintaining higher velocities and lower pressures compared to the lower surface. Pressure levels are notably higher at the leading and

trailing edges across all angles. Throughout the analysed AOAs, the upper surface remains a high-velocity region, while the lower surface exhibits lower velocities and moderate pressure. The consistent low-pressure region on the upper surface and the moderate pressure on the lower surface, particularly at the leading edge, indicate that the airfoil is designed to optimize lift while minimizing drag

REFERENCES

1. “Study of flow over supercritical airfoil and it’s comparison with NACA airfoil” by Shiva Sharma.
2. J. H. B. Smith, “Introductory remarks,” The Aeronautical Journal.
3. "Fundamentals of Aerodynamics" by John D. Anderson Jr.
4. Supercritical airfoil by “Wikipedia”.
5. Anderson, J. D. (2010). Fundamentals of Aerodynamics (5th ed.). McGraw-Hill Education.
6. Bertin, J. J., & Smith, M. L. (2013). Aerodynamics for Engineers (5th ed.). Pearson.
7. Whitcomb, R. T. (1976). The Supercritical Airfoil. Journal of Aircraft, 13(6), 469-475.
8. “Study flow over supercritical airfoil and it’s comparison with NACA airfoil” by Shiva Sharma.
9. J. H. B. Smith, “Introductory remarks,” The Aeronautical Journal.